

Performance Analysis of a Hybrid Downlink-Uplink Cooperative NOMA Scheme

(Invited Paper)

Zhiqiang Wei, Linglong Dai, Derrick Wing Kwan Ng, and Jinhong Yuan

Abstract—This paper proposes a novel hybrid downlink-uplink cooperative NOMA (HDU-CNOMA) scheme to achieve a better tradeoff between spectral efficiency and signal reception reliability than the conventional cooperative NOMA schemes. In particular, the proposed scheme enables the strong user to perform a cooperative transmission and an interference-free uplink transmission simultaneously during the cooperative phase, at the expense of a slightly decrease in signal reception reliability at the weak user. We analyze the outage probability, diversity order, and outage throughput of the proposed scheme. Simulation results not only confirm the accuracy of the developed analytical results, but also unveil the spectral efficiency gains achieved by the proposed scheme over a baseline cooperative NOMA scheme and a non-cooperative NOMA scheme.

I. INTRODUCTION

Recently, non-orthogonal multiple access (NOMA) has drawn a lot of attentions as an important enabling technique to fulfill the challenging requirements of the fifth-generation (5G) communication systems, such as massive connectivity, high spectral efficiency, and ultra-low latency [1], [2], [3]. In the literature, different schemes, such as power domain NOMA and code domain NOMA, have been proposed to facilitate multiuser multiplexing [3]. Power domain NOMA is particularly appealing as it can be integrated with the existing fourth-generation communication systems. The fundamental idea of power domain NOMA is to exploit the power domain for multiuser multiplexing via using superposition coding at transmitters and successive interference cancellation (SIC) at receivers [4]. In particular, NOMA allows a strong user (with better channel condition) concurrently accessing the spectrum resources assigned for a weak user (with worse channel condition) to increase the system spectral efficiency. To alleviate the inter-user interference (IUI) at the weak user, a larger amount of power is allocated to the weak user while a smaller fraction of power is provided for the strong user. Meanwhile, SIC technique is adopted at the receiver of the strong user to remove the IUI. It has been shown that NOMA provides substantial performance gains over conventional orthogonal multiple access (OMA) in terms of spectral efficiency [5], [6], [7] and fairness [8], [9].

In wireless communications, the system performance is significantly limited by channel fading raised from multi-path propagations. This issue is more prominent in NOMA

scenarios. Specifically, weak users become more vulnerable to channel fading due to not only the severe path loss, but also the IUI caused by the simultaneous communication to strong users. Traditionally, cooperative diversity is an effective technique to combat channel fading in wireless networks [10]. Among different cooperative strategies proposed in the literature [11], [12], [13], cooperative relaying is an attractive technique to increase the range of communication systems and to enhance the link reliability without incurring the high cost of additional base station deployment. Therefore, a cooperative NOMA (CNOMA) scheme was proposed in [14] to improve the signal reception reliability for the weak user by exploiting the prior information obtained at the strong user during SIC process. Particularly, in addition to the downlink NOMA transmission phase, the strong user acts as a decode-and-forward (DF) relay to deliver messages to the weak user in the cooperative phase. The extensions of this scheme to multiple-antenna relaying networks and full-duplex relaying networks were investigated in [15] and [16], respectively. Note that the aforementioned CNOMA schemes enhance the signal reception reliability at the price of reduced spectral efficiency due to the duplicate transmission during the cooperative phase. More recently, a non-orthogonal relaying strategy is applied in CNOMA systems to improve the spectral efficiency, where a base station (BS) and a relay transmit their messages at the same time in the same frequency. Nevertheless, a dedicated relay is required in most of existing schemes [17], [18]. Also, these schemes do not fully exploit the BS in the cooperative phase which lead to potential loss in spectral efficiency.

In this paper, we propose a new hybrid downlink-uplink CNOMA (HDU-CNOMA) scheme to improve the spectral efficiency. Different from the conventional CNOMA scheme [14], our proposed scheme enables the uplink transmission from the strong user to the BS during the cooperative phase. Hence, it is expected that our proposed scheme is able to improve the achievable system sum rate at a price of a slightly decrease in the signal reception reliability at the weak user. Besides, we derive the closed-form expressions of the system outage probability and the diversity orders to characterize the performance of the proposed scheme. Numerical results are shown to verify our analytical results and to demonstrate the effectiveness of our proposed scheme.

II. SYSTEM MODEL

Consider a communication scenario including downlink and uplink transmission with one BS and two users¹, as shown

¹The extension to the case with more than two users is straightforward by following a similar approach as [14].

Zhiqiang Wei, Derrick Wing Kwan Ng, and Jinhong Yuan are with the School of Electrical Engineering and Telecommunications, the University of New South Wales, Australia (email: zhiqiang.wei@student.unsw.edu.au; w.k.ng@unsw.edu.au; j.yuan@unsw.edu.au). Linglong Dai is with the Department of Electronic Engineering, Tsinghua University, China (email: daill@tsinghua.edu.cn). Derrick is supported under Australian Research Council's Scheme Discovery Early Career Researcher Award funding scheme (project number DE170100137).

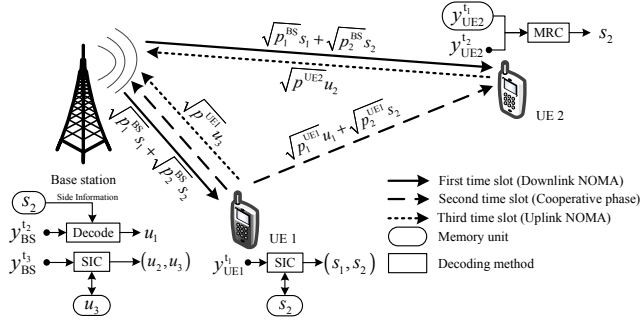


Fig. 1. The proposed HDU-CNOMA scheme with one BS and two users.

in Figure 1. All the transceivers are equipped with a single antenna and operate in half-duplex mode, i.e., they cannot transmit and receive a signal at the same time in the same frequency. Furthermore, we assume a time division duplex (TDD) protocol for facilitating downlink and uplink transmission. We denote $h_{BS,UE1}$ as the channel coefficient between the BS and user 1 (UE 1), $h_{BS,UE2}$ as the channel coefficient between the BS and user 2 (UE 2), and $h_{UE1,UE2}$ as the channel coefficient between UE 1 and UE 2. We assume that perfect channel state information (CSI) is available at receivers for signal detection, while only statistical CSI is available at transmitters. All the links considered here are assumed to experience independent quasi-static fading, where the channel coefficients are constant for each time slot but vary independently between different time slots for different links. Besides, we assume that the channel coefficients are Rayleigh distributed: $h_\delta \sim \mathcal{CN}(0, \beta_\delta)$, $\delta \in \{(BS, UE1), (BS, UE2), (UE1, UE2)\}$, where $\mathcal{CN}(0, \beta_\delta)$ denotes the circularly symmetric complex Gaussian distribution with zero-mean and variance β_δ , and the variance β_δ captures the effect of large scale fading for the link δ . Then, the cumulative distribution function (CDF) and probability density function (PDF) for the channel gain of link δ , i.e., $|h_\delta|^2$, are given by

$$F_{|h_\delta|^2}(x) = 1 - \exp\left(-\frac{x}{\beta_\delta}\right), \quad x \geq 0, \quad \text{and} \quad (1)$$

$$f_{|h_\delta|^2}(x) = \frac{1}{\beta_\delta} \exp\left(-\frac{x}{\beta_\delta}\right), \quad x \geq 0, \quad (2)$$

respectively, where $|\cdot|$ denotes the absolute value of a complex scalar. Meanwhile, we consider the user with the larger β_δ as the strong user and without loss of generality, we assume $\beta_{BS,UE1} > \beta_{BS,UE2}$. In other words, UE 1 is selected to perform SIC and to assist UE 2 in our proposed scheme[19], [20]. Note that this may not be the optimal SIC decoding order to minimize the system outage probability under statistical CSI assumption[19], [21], because $\beta_{BS,UE1} > \beta_{BS,UE2}$ does not guarantee $|h_{BS,UE1}|^2 > |h_{BS,UE2}|^2$. However, it is a simple but effective strategy under statistical CSI[19]. To facilitate our performance analysis, we focus on this specific scheme with UE 1 as the strong user and serving as a relay to assist UE 2.

As shown in Figure 1 and Figure 2(a), in our proposed HDU-CNOMA scheme, one time frame is partitioned into three time slots with equal duration for downlink NOMA

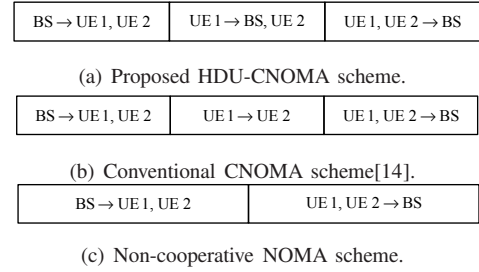


Fig. 2. Illustrations for: a) proposed HDU-CNOMA scheme; b) conventional CNOMA scheme[14]; c) non-cooperative NOMA scheme.

phase, cooperative phase, and uplink NOMA phase. Note that fixed power allocation is adopted for in this paper. Although optimizing the power allocation during different phases can further improve the performance of our proposed scheme, it is beyond the scope of this paper and will be considered in our future work. In the following, we present our proposed scheme.

A. Proposed HDU-CNOMA Scheme

In the first time slot, i.e., the downlink NOMA phase, the transmitted signal from the BS is given by

$$x_{BS}^{t_1} = \sqrt{\alpha_{UE1}^{t_1} P_0} s_1 + \sqrt{\alpha_{UE2}^{t_1} P_0} s_2, \quad (3)$$

where superscript t_1 denotes the 1-st time slot, P_0 denotes the maximum transmit power for the BS, s_1 and s_2 denote the modulated downlink symbols for UE 1 and UE 2, respectively, and $\alpha_{UE1}^{t_1}$ and $\alpha_{UE2}^{t_1}$ denote the power allocation factors for UE 1 and UE 2 in t_1 , respectively. According to the NOMA protocol[5], we allocate more power to the weak user, thus we have $\alpha_{UE1}^{t_1} \leq \alpha_{UE2}^{t_1}$ and $\alpha_{UE1}^{t_1} + \alpha_{UE2}^{t_1} = 1$. For notational simplicity, we assume the same maximum transmit power for the BS, UE 1, and UE 2 in our model². Subsequently, the received signals at UE 1 and UE 2 in t_1 are given by

$$y_{UE1}^{t_1} = h_{BS,UE1} \left(\sqrt{\alpha_{UE1}^{t_1} P_0} s_1 + \sqrt{\alpha_{UE2}^{t_1} P_0} s_2 \right) + z_{UE1} \quad \text{and} \quad (4)$$

$$y_{UE2}^{t_1} = h_{BS,UE2} \left(\sqrt{\alpha_{UE1}^{t_1} P_0} s_1 + \sqrt{\alpha_{UE2}^{t_1} P_0} s_2 \right) + z_{UE2}, \quad (5)$$

respectively, where $z_{UE1} \sim \mathcal{CN}(0, \sigma^2)$ and $z_{UE2} \sim \mathcal{CN}(0, \sigma^2)$ denote the additive white Gaussian noise (AWGN) at UE 1 and UE 2, respectively, with the same noise power σ^2 .

Then, UE 1 will first decode message of UE 2 s_2 , subtract it from its observation $y_{UE1}^{t_1}$, and then decode its own message s_1 . The signal-to-interference-plus-noise ratio (SINR) for UE 1 to decode the message of UE 2 is given by

$$\text{SINR}_{UE1,UE2}^{t_1} = \frac{|h_{BS,UE1}|^2 \alpha_{UE2}^{t_1}}{|h_{BS,UE1}|^2 \alpha_{UE1}^{t_1} + 1/\rho}. \quad (6)$$

where $\rho = \frac{P_0}{\sigma^2}$ denotes the transmit signal-to-noise ratio (SNR). For a given target data rate of downlink transmission of UE 2, R_{UE2}^{DL} , if $\frac{1}{3} \log_2 \left(1 + \text{SINR}_{UE1,UE2}^{t_1} \right) \geq R_{UE2}^{DL}$, the message s_2 is decodable and can be cancelled at UE 1,

²Note that it is straightforward to extend the results of this paper to the case with different transmit powers.

otherwise the SIC process is failed. Note that a pre-log factor of $\frac{1}{3}$ is introduced which takes into account the loss of spectral efficiency as one time frame is partitioned into three time slots. Meanwhile, we assume that UE 1 will not decode its own message s_1 if the SIC process is failed. Therefore, with a successful SIC, the SINR for UE 1 to decode its own messages is given by

$$\text{SINR}_{\text{UE1}}^{t_1} = |h_{\text{BS,UE1}}|^2 \alpha_{\text{UE1}}^{t_1} \rho. \quad (7)$$

On the other hand, UE 2 will directly decode its own message s_2 by treating the signal of UE 1 as noise. Thereby, the SINR for UE 2 to decode its own message is given by

$$\text{SINR}_{\text{UE2}}^{t_1} = \frac{|h_{\text{BS,UE2}}|^2 \alpha_{\text{UE2}}^{t_1}}{|h_{\text{BS,UE2}}|^2 \alpha_{\text{UE1}}^{t_1} + 1/\rho}. \quad (8)$$

In the second time slot t_2 , i.e., the cooperative phase, UE 1 will broadcast the superimposed signal of s_2 and u_1 , where s_2 is the message for UE 2 obtained during SIC process in the first time slot and u_1 is its own message for uplink transmission. The transmitted signal from UE 1 in the second time slot is given by

$$x_{\text{UE1}}^{t_2} = \sqrt{\alpha_{\text{BS}}^{t_2} P_0} u_1 + \sqrt{\alpha_{\text{UE2}}^{t_2} P_0} s_2, \quad (9)$$

where $\alpha_{\text{BS}}^{t_2}$ and $\alpha_{\text{UE2}}^{t_2}$ denote the power allocation factors for the messages for the BS and UE 2 in t_2 , respectively, with $\alpha_{\text{BS}}^{t_2} + \alpha_{\text{UE2}}^{t_2} = 1$. As a result, the received signal at the BS and UE 2 in t_2 are given by

$$y_{\text{BS}}^{t_2} = h_{\text{BS,UE1}} \left(\sqrt{\alpha_{\text{BS}}^{t_2} P_0} u_1 + \sqrt{\alpha_{\text{UE2}}^{t_2} P_0} s_2 \right) + z_{\text{BS}} \quad \text{and} \quad (10)$$

$$y_{\text{UE2}}^{t_2} = h_{\text{UE1,UE2}} \left(\sqrt{\alpha_{\text{BS}}^{t_2} P_0} u_1 + \sqrt{\alpha_{\text{UE2}}^{t_2} P_0} s_2 \right) + z_{\text{UE2}}, \quad (11)$$

respectively, where $z_{\text{BS}} \sim \mathcal{CN}(0, \sigma^2)$ denotes the AWGN at the BS.

Since the BS knows exactly the downlink message s_2 in advance, it can subtract it directly from its observation $y_{\text{BS}}^{t_2}$ and decode the uplink message u_1 . In other words, the downlink message s_2 stored at the BS serves as a piece of side information which benefits the decoding of the uplink message u_1 . Therefore, our proposed scheme enables an interference-free uplink transmission and can significantly increase the system spectral efficiency. On the other hand, compared to the conventional CNOMA scheme, it is expected that there is a slightly decrease in the signal reception reliability at UE 2 as a portion of transmit power at UE 1, $\sqrt{\alpha_{\text{UE2}}^{t_2} P_0}$, is used for uplink transmission for UE 1. In fact, allocating a small fraction of power for the uplink transmission of UE 1 can enable a noticeable system performance gain in spectral efficiency owing to its good channel condition and the interference-free transmission. Therefore, in the proposed scheme, one can use the power allocation factor $\alpha_{\text{UE2}}^{t_2}$ to control the tradeoff between system spectral efficiency and signal reception reliability. Note that the conventional CNOMA scheme is a subcase of our proposed scheme which can be obtained by setting $\alpha_{\text{UE2}}^{t_2} = 0$. More importantly, unlike the SIC process in t_1 at UE 1, the downlink message s_2 can always

be cancelled disregard the target data rate of the downlink transmission of UE 2.

At the BS, after eliminating s_2 from $y_{\text{BS}}^{t_2}$, the SINR for the BS to decode the uplink message u_1 is given by

$$\text{SINR}_{\text{BS,UE1}}^{t_2} = |h_{\text{BS,UE1}}|^2 \alpha_{\text{BS}}^{t_2} \rho. \quad (12)$$

On the other hand, at UE 2, the maximum ratio combining (MRC) is adopted to decode the message s_2 from two independent observations $y_{\text{UE2}}^{t_1}$ and $y_{\text{UE2}}^{t_2}$ with weights

$\frac{h_{\text{BS,UE2}}^* \sqrt{\alpha_{\text{UE2}}^{t_1} P_0}}{|h_{\text{BS,UE2}}|^2 \alpha_{\text{UE1}}^{t_1} P_0 + \sigma^2}$ and $\frac{h_{\text{UE1,UE2}}^* \sqrt{\alpha_{\text{UE2}}^{t_2} P_0}}{|h_{\text{UE1,UE2}}|^2 \alpha_{\text{BS}}^{t_2} P_0 + \sigma^2}$, respectively, where $*$ denotes the conjugate operation. Therefore, the SINR for UE 2 to decode s_2 with MRC is given by

$$\text{SINR}_{\text{UE2-MRC}}^{t_1, t_2} = \text{SINR}_{\text{UE2}}^{t_1} + \text{SINR}_{\text{UE2}}^{t_2}, \quad (13)$$

where $\text{SINR}_{\text{UE2}}^{t_2}$ denotes the SINR for UE 2 to decode s_2 in t_2 , and it is given by

$$\text{SINR}_{\text{UE2}}^{t_2} = \frac{|h_{\text{UE1,UE2}}|^2 \alpha_{\text{UE2}}^{t_2}}{|h_{\text{UE1,UE2}}|^2 \alpha_{\text{BS}}^{t_2} + 1/\rho}. \quad (14)$$

In the third time slot t_3 , i.e., the uplink NOMA phase, UE 1 and UE 2 transmit their uplink messages u_3 and u_2 to the BS simultaneously. Note that the different large scale fading experienced by both users results in different received signal powers from UE 1 and UE 2, which can inherently facilitate the SIC process. Therefore, we simply assume that both users transmit their messages with their maximum transmit powers for notation simplification. The received signal at the BS in the third time slot is given by

$$y_{\text{BS}}^{t_3} = h_{\text{BS,UE1}} \sqrt{P_0} u_3 + h_{\text{BS,UE2}} \sqrt{P_0} u_2 + z_{\text{BS}}. \quad (15)$$

According to the uplink NOMA principle[22], the BS will first decode the user with higher received power. If $|h_{\text{BS,UE1}}|^2 \geq |h_{\text{BS,UE2}}|^2$, the SINR for the BS to decode the uplink messages of UE 1 and UE 2 are given by

$$\text{SINR}_{\text{BS,UE1}}^{t_3} = \frac{|h_{\text{BS,UE1}}|^2}{|h_{\text{BS,UE2}}|^2 + 1/\rho} \quad \text{and} \quad (16)$$

$$\text{SINR}_{\text{BS,UE2}}^{t_3} = |h_{\text{BS,UE2}}|^2 \rho, \quad (17)$$

respectively. On the other hand, if $|h_{\text{BS,UE1}}|^2 < |h_{\text{BS,UE2}}|^2$, the SINR for the BS to decode the uplink messages of UE 1 and UE 2 are given by

$$\overline{\text{SINR}}_{\text{BS,UE1}}^{t_3} = |h_{\text{BS,UE1}}|^2 \rho \quad \text{and} \quad (18)$$

$$\overline{\text{SINR}}_{\text{BS,UE2}}^{t_3} = \frac{|h_{\text{BS,UE2}}|^2}{|h_{\text{BS,UE1}}|^2 + 1/\rho}, \quad (19)$$

respectively. Here, we assume that the BS will not decode the message of the user with lower received power if the SIC process is failed.

Remark 1: For comparison, two baseline schemes, the conventional CNOMA scheme and the non-cooperative NOMA scheme, are illustrated in Figure 2(b) and Figure 2(c), respectively. For a fair comparison, the time duration of the frame for all the schemes illustrated in Figure 2 are identical. Similar to our proposed scheme, the CNOMA scheme also requires three time slots to accomplish the downlink transmission,

cooperative transmission, and uplink transmission. Different from the CNOMA scheme, UE 1 in our proposed scheme will broadcast the superposition of downlink symbols for UE 2 and uplink symbols of itself in the cooperative phase. In contrast, the non-cooperative NOMA scheme needs two time slots for downlink NOMA and uplink NOMA transmissions.

III. PERFORMANCE ANALYSIS

To characterize the reception reliability and system spectral efficiency of our proposed scheme, three performance metrics are discussed in this section. Firstly, we analyze the outage probability for individual link for a given the target data rate, from which the diversity order achieved by the proposed scheme is obtained. Then, the system outage throughput is derived to demonstrate the improvement of spectral efficiency.

Given the target data rate for downlink and uplink transmissions of UE 1 and UE 2 as R_{UE1}^{DL} , R_{UE2}^{DL} , R_{UE1}^{UL} , R_{UE2}^{UL} , respectively, an outage occurs when the achievable rate is less than that of the corresponding target data rate. Accordingly, the outage probability of downlink and uplink transmissions of UE 1 and UE 2 are given by (20)-(24) at the top of next page. Note that we assume the same target data rate R_{UE1}^{UL} for the uplink transmissions of UE 1 in t_2 and t_3 . Correspondingly, their outage probability are denoted as $P_{out, t_2}^{UE1, UL}$ and $P_{out, t_3}^{UE1, UL}$, respectively.

The outage probability of UE 1 for downlink NOMA transmission has been derived in [17] as follows:

$$P_{out}^{UE1, DL} = \begin{cases} 1 - \exp\left(-\frac{\phi_1}{\beta_{BS, UE1}\rho}\right), & \text{if } \alpha_{UE2}^{t_1} - \alpha_{UE1}^{t_1} \gamma_{UE2}^{DL} > 0 \\ 1, & \text{otherwise} \end{cases} \quad (25)$$

where $\phi_1 = \max\left\{\frac{\gamma_{UE2}^{DL}}{(\alpha_{UE2}^{t_1} - \alpha_{UE1}^{t_1} \gamma_{UE2}^{DL})}, \frac{\gamma_{UE1}^{DL}}{\alpha_{UE1}^{t_1}}\right\}$, $\gamma_{UE1}^{DL} = 2^{3R_{UE1}^{DL}} - 1$, and $\gamma_{UE2}^{DL} = 2^{3R_{UE2}^{DL}} - 1$. It is notable that the power allocation factors should satisfy $\alpha_{UE2}^{t_1} - \alpha_{UE1}^{t_1} \gamma_{UE2}^{DL} > 0$, otherwise $P_{out}^{UE1, DL}$ will always be one.

Based on (21), the outage probability of UE 2 for downlink NOMA transmission is derived as (26) at the top of next page, where Q_1 and Q_2 can be easily obtained as

$$Q_1 = 1 - \exp\left(-\frac{\phi_2}{\beta_{BS, UE1}\rho}\right) \text{ and } Q_2 = 1 - \exp\left(-\frac{\phi_2}{\beta_{BS, UE2}\rho}\right), \quad (27)$$

respectively, and $\phi_2 = \frac{\gamma_{UE2}^{DL}}{(\alpha_{UE2}^{t_1} - \alpha_{UE1}^{t_1} \gamma_{UE2}^{DL})}$. Again, the prerequisite $\alpha_{UE2}^{t_1} - \alpha_{UE1}^{t_1} \gamma_{UE2}^{DL} > 0$ should be satisfied, otherwise $P_{out}^{UE2, DL}$ will always be one.

For Q_3 , we first derive the distributions of $\text{SINR}_{UE2}^{t_1}$ and $\text{SINR}_{UE2}^{t_2}$, respectively, and then obtain Q_3 via the following integration:

$$Q_3 = \int \int_{\text{SINR}_{UE2}^{t_1} + \text{SINR}_{UE2}^{t_2} < \gamma_{UE2}^{DL}} f_{\text{SINR}_{UE2}^{t_2}}(x) f_{\text{SINR}_{UE2}^{t_1}}(y) dy dx. \quad (28)$$

The CDF of $\text{SINR}_{UE2}^{t_1}$ is defined as

$$F_{\text{SINR}_{UE2}^{t_1}}(x) = \Pr\{\text{SINR}_{UE2}^{t_1} < x\}, \quad (29)$$

thereby, if $0 < x < \frac{\alpha_{UE2}^{t_1}}{\alpha_{UE1}^{t_1}}$, the CDF and PDF of $\text{SINR}_{UE2}^{t_1}$ are given by

$$F_{\text{SINR}_{UE2}^{t_1}}(x) = F_{|h_{BS, UE2}|^2} \left(\frac{x}{(\alpha_{UE2}^{t_1} - \alpha_{UE1}^{t_1} x)\rho} \right) \text{ and} \quad (30)$$

$$f_{\text{SINR}_{UE2}^{t_1}}(x) = f_{|h_{BS, UE2}|^2} \left(\frac{x}{(\alpha_{UE2}^{t_1} - \alpha_{UE1}^{t_1} x)\rho} \right) \frac{\alpha_{UE2}^{t_1}}{(\alpha_{UE2}^{t_1} - \alpha_{UE1}^{t_1} x)^2 \rho}, \quad (31)$$

respectively. Similarly, for $0 < x < \frac{\alpha_{UE2}^{t_2}}{\alpha_{BS}^{t_2}}$, the CDF and PDF of $\text{SINR}_{UE2}^{t_2}$ can be obtained as

$$F_{\text{SINR}_{UE2}^{t_2}}(x) = F_{|h_{UE1, UE2}|^2} \left(\frac{x}{(\alpha_{UE2}^{t_2} - \alpha_{BS}^{t_2} x)\rho} \right) \text{ and} \quad (32)$$

$$f_{\text{SINR}_{UE2}^{t_2}}(x) = f_{|h_{UE1, UE2}|^2} \left(\frac{x}{(\alpha_{UE2}^{t_2} - \alpha_{BS}^{t_2} x)\rho} \right) \frac{\alpha_{UE2}^{t_2}}{(\alpha_{UE2}^{t_2} - \alpha_{BS}^{t_2} x)^2 \rho}, \quad (33)$$

respectively. Then, Q_3 can be obtained by solving:

$$Q_3 = \int_0^{\phi_3} \int_0^{\gamma_{UE2}^{DL} - x} f_{\text{SINR}_{UE2}^{t_2}}(x) f_{\text{SINR}_{UE2}^{t_1}}(y) dy dx, \quad (34)$$

where $\phi_3 = \min\left(\gamma_{UE2}^{DL}, \frac{\alpha_{UE2}^{t_2}}{\alpha_{BS}^{t_2}}\right)$.

It is difficult to directly solve the above integration. To obtain more insights from $P_{out}^{UE2, DL}$ in (26), we apply the Gauss-Chebyshev integration[23] to obtain Q_3 via a closed-form approximation as follows³:

$$Q_3 \approx F_{\text{SINR}_{UE2}^{t_2}}(\phi_3) - \frac{\alpha_{UE2}^{t_2} \phi_3}{2\beta_{UE1, UE2}\rho} \sum_{i=1}^n \frac{\pi}{n} \left| \sin \frac{2i-1}{2n} \pi \right| g(l_i), \quad (35)$$

where n is the number of Gauss-Chebyshev integral approximation terms, $l_i = \frac{\phi_3}{2} + \frac{\phi_3}{2} \cos \frac{2i-1}{2n} \pi$, and $g(x)$ is given by

$$g(x) = \frac{1}{(\alpha_{UE2}^{t_2} - \alpha_{BS}^{t_2})^2} \exp\left(-\frac{x}{(\alpha_{UE2}^{t_2} - \alpha_{BS}^{t_2} x) \beta_{UE1, UE2}\rho} - \frac{(\gamma_{UE2}^{DL} - x)}{(\alpha_{UE2}^{t_1} - \alpha_{UE1}^{t_1} \gamma_{UE2}^{DL} + \alpha_{UE1}^{t_1} x) \beta_{BS, UE2}\rho}\right). \quad (36)$$

Substitute Q_1 , Q_2 , and Q_3 into (26), if $\alpha_{UE2}^{t_1} - \alpha_{UE1}^{t_1} \gamma_{UE2}^{DL} > 0$, the outage probability for the downlink transmission of UE 2 can be derived as (37) at the top of next page.

In t_2 , since the interference of the weak user can be perfectly cancelled at the BS, the outage probability of UE 1 for uplink NOMA transmission can be easily obtained by

$$P_{out, t_2}^{UE1, UL} = 1 - \exp\left(-\frac{\gamma_{UE1}^{UL}}{\beta_{BS, UE1} \alpha_{BS}^{t_2} \rho}\right), \quad (38)$$

where $\gamma_{UE1}^{UL} = 2^{3R_{UE1}^{UL}} - 1$.

For the uplink NOMA transmission phase, the outage probability is complicated since the integral area in (23) and (24) depends on the target data rates of uplink transmissions of both

³The tightness of the adopted approximation will be verified in the simulation section.

$$P_{\text{out}}^{\text{UE1, DL}} = \Pr \left\{ \frac{1}{3} \log_2 (1 + \text{SINR}_{\text{UE1, UE2}}^{t_1}) < R_{\text{UE2}}^{\text{DL}} \right\} + \Pr \left\{ \frac{1}{3} \log_2 (1 + \text{SINR}_{\text{UE1, UE2}}^{t_1}) \geq R_{\text{UE2}}^{\text{DL}}, \frac{1}{3} \log_2 (1 + \text{SINR}_{\text{UE1}}^{t_1}) < R_{\text{UE1}}^{\text{DL}} \right\}, \quad (20)$$

$$P_{\text{out}}^{\text{UE2, DL}} = \Pr \left\{ \frac{1}{3} \log_2 (1 + \text{SINR}_{\text{UE1, UE2}}^{t_1}) < R_{\text{UE2}}^{\text{DL}}, \frac{1}{3} \log_2 (1 + \text{SINR}_{\text{UE2}}^{t_1}) < R_{\text{UE2}}^{\text{DL}} \right\} + \Pr \left\{ \frac{1}{3} \log_2 (1 + \text{SINR}_{\text{UE1, UE2}}^{t_1}) \geq R_{\text{UE2}}^{\text{DL}}, \frac{1}{3} \log_2 (1 + \text{SINR}_{\text{UE2}}^{t_1, t_2}) < R_{\text{UE2}}^{\text{DL}} \right\}, \quad (21)$$

$$P_{\text{out}, t_2}^{\text{UE1, UL}} = \Pr \left\{ \frac{1}{3} \log_2 (1 + \text{SINR}_{\text{BS, UE1}}^{t_2}) < R_{\text{UE1}}^{\text{UL}} \right\}, \quad (22)$$

$$P_{\text{out}, t_3}^{\text{UE1, UL}} = \Pr \left\{ |h_{\text{BS, UE1}}|^2 \geq |h_{\text{BS, UE2}}|^2, \frac{1}{3} \log_2 (1 + \text{SINR}_{\text{BS, UE1}}^{t_3}) < R_{\text{UE1}}^{\text{UL}} \right\} + \Pr \left\{ |h_{\text{BS, UE1}}|^2 < |h_{\text{BS, UE2}}|^2, \frac{1}{3} \log_2 (1 + \overline{\text{SINR}}_{\text{BS, UE2}}^{t_3}) < R_{\text{UE2}}^{\text{UL}} \right\} + \Pr \left\{ |h_{\text{BS, UE1}}|^2 < |h_{\text{BS, UE2}}|^2, \frac{1}{3} \log_2 (1 + \overline{\text{SINR}}_{\text{BS, UE2}}^{t_3}) \geq R_{\text{UE2}}^{\text{UL}}, \frac{1}{3} \log_2 (1 + \overline{\text{SINR}}_{\text{BS, UE1}}^{t_3}) < R_{\text{UE1}}^{\text{UL}} \right\}, \quad (23)$$

$$P_{\text{out}}^{\text{UE2, UL}} = \Pr \left\{ |h_{\text{BS, UE2}}|^2 \geq |h_{\text{BS, UE1}}|^2, \frac{1}{3} \log_2 (1 + \overline{\text{SINR}}_{\text{BS, UE2}}^{t_3}) < R_{\text{UE2}}^{\text{UL}} \right\} + \Pr \left\{ |h_{\text{BS, UE2}}|^2 < |h_{\text{BS, UE1}}|^2, \frac{1}{3} \log_2 (1 + \text{SINR}_{\text{BS, UE1}}^{t_3}) < R_{\text{UE1}}^{\text{UL}} \right\} + \Pr \left\{ |h_{\text{BS, UE2}}|^2 < |h_{\text{BS, UE1}}|^2, \frac{1}{3} \log_2 (1 + \text{SINR}_{\text{BS, UE1}}^{t_3}) \geq R_{\text{UE1}}^{\text{UL}}, \frac{1}{3} \log_2 (1 + \text{SINR}_{\text{BS, UE2}}^{t_3}) < R_{\text{UE2}}^{\text{UL}} \right\}. \quad (24)$$

$$P_{\text{out}}^{\text{UE2, DL}} = \underbrace{\Pr \left\{ \frac{1}{3} \log_2 (1 + \text{SINR}_{\text{UE1, UE2}}^{t_1}) < R_{\text{UE2}}^{\text{DL}} \right\}}_{Q_1} \underbrace{\Pr \left\{ \frac{1}{3} \log_2 (1 + \text{SINR}_{\text{UE2, UE2}}^{t_1}) < R_{\text{UE2}}^{\text{DL}} \right\}}_{Q_2} + \underbrace{\Pr \left\{ \frac{1}{3} \log_2 (1 + \text{SINR}_{\text{UE1, UE2}}^{t_1}) \geq R_{\text{UE2}}^{\text{DL}} \right\}}_{1-Q_1} \underbrace{\Pr \left\{ \frac{1}{3} \log_2 (1 + \text{SINR}_{\text{UE2, UE2}}^{t_1, t_2}) < R_{\text{UE2}}^{\text{DL}} \right\}}_{Q_3}. \quad (26)$$

$$P_{\text{out}}^{\text{UE2, DL}} = \left(1 - \exp \left(-\frac{\phi_2}{\beta_{\text{BS, UE1}} \rho} \right) \right) \left(1 - \exp \left(-\frac{\phi_2}{\beta_{\text{BS, UE2}} \rho} \right) \right) - \exp \left(-\frac{\phi_2}{\beta_{\text{BS, UE1}} \rho} \right) \cdot \left\{ 1 - \exp \left(-\frac{\phi_3}{\beta_{\text{UE1, UE2}} (\alpha_{\text{UE2}}^{t_2} - \alpha_{\text{BS}}^{t_2} \phi_3)} \right) - \frac{\alpha_{\text{UE2}}^{t_2} \phi_3}{2\beta_{\text{UE1, UE2}} \rho} \sum_{i=1}^n \frac{\pi}{n} \left| \sin \left(\frac{2i-1}{2n} \pi \right) \right| g(l_i) \right\}. \quad (37)$$

users. As a compromise solution, we focus on high data rate applications, e.g. $R_{\text{UE1}}^{\text{UL}} > \frac{1}{3}$ bit/s/Hz and $R_{\text{UE2}}^{\text{UL}} > \frac{1}{3}$ bit/s/Hz. The closed-form outage probability of UE 1 for uplink NOMA transmission is derived in (39) at the top of next page, wherein $\gamma_{\text{UE2}}^{\text{UL}} = 2^{3R_{\text{UE2}}^{\text{UL}}} - 1$. Note that (a) in (39) holds when $R_{\text{UE1}}^{\text{UL}} > \frac{1}{3}$ bit/s/Hz and $R_{\text{UE2}}^{\text{UL}} > \frac{1}{3}$ bit/s/Hz. Similarly, the outage probability of the uplink transmission of UE 2 can be given by (40) at the top of next page.

Now, we analyze the diversity order for each link for our proposed scheme to obtain more insights into the system outage performance. The diversity order is defined as $d = \lim_{\rho \rightarrow \infty} \frac{-\log P_{\text{out}}}{\log \rho}$ [24] and the results are summarized in the following lemma.

Lemma 1: By using the high SNR approximation, i.e., $1 - \exp(-\frac{x}{\rho}) \approx \frac{x}{\rho}$ [14], we obtain the diversity order for each communication link as:

$$d_{\text{out}}^{\text{UE1, DL}} = 1, d_{\text{out}}^{\text{UE2, DL}} = 2, d_{\text{out}, t_2}^{\text{UE1, UL}} = 1, \quad (41)$$

$$d_{\text{out}, t_3}^{\text{UE1, UL}} = 0, \text{ and } d_{\text{out}}^{\text{UE2, UL}} = 0. \quad (42)$$

The diversity order for the downlink transmission of UE 1 is one. Besides, the diversity order for the downlink transmission of UE 2 is two since there are two independent observations of the downlink messages of UE 2 in our proposed scheme. On the other hand, we obtain an uplink transmission for UE 1 with a diversity order of one via the superposition transmission during the cooperative phase. Interestingly, the diversity order for uplink NOMA transmission is zero, which implies that there is an error floor for the outage probability at high transmit SNR ρ . This is due to the lack of adaptive power control for uplink NOMA transmission leading to a significant IUI in the high transmit SNR regime⁴.

On the other hand, as all the nodes transmit their information at their fixed target data rates and the system throughput is determined by the outage probability. Therefore, to evaluate the spectral efficiency of our proposed scheme, we define the system outage throughput in (43) at the top of this page.

⁴We note that the error floor inherently exists in the uplink of cooperative NOMA schemes with fixed power allocation [22], [25].

$$\begin{aligned}
P_{\text{out}, t_3}^{\text{UE1, UL}} &= \Pr \left\{ |h_{\text{BS, UE1}}|^2 \geq |h_{\text{BS, UE2}}|^2, |h_{\text{BS, UE1}}|^2 - |h_{\text{BS, UE2}}|^2 \gamma_{\text{UE1}}^{\text{UL}} < \gamma_{\text{UE1}}^{\text{UL}} / \rho \right\} \\
&+ \Pr \left\{ |h_{\text{BS, UE1}}|^2 < |h_{\text{BS, UE2}}|^2, |h_{\text{BS, UE2}}|^2 - |h_{\text{BS, UE1}}|^2 \gamma_{\text{UE2}}^{\text{UL}} < \gamma_{\text{UE2}}^{\text{UL}} / \rho \right\} \\
&+ \Pr \left\{ |h_{\text{BS, UE1}}|^2 < |h_{\text{BS, UE2}}|^2, |h_{\text{BS, UE2}}|^2 - |h_{\text{BS, UE1}}|^2 \gamma_{\text{UE2}}^{\text{UL}} \geq \gamma_{\text{UE2}}^{\text{UL}} / \rho, |h_{\text{BS, UE1}}|^2 < \gamma_{\text{UE1}}^{\text{UL}} / \rho \right\} \\
&\stackrel{(a)}{=} 1 - \Pr \left\{ |h_{\text{BS, UE1}}|^2 - |h_{\text{BS, UE2}}|^2 \gamma_{\text{UE1}}^{\text{UL}} \geq \gamma_{\text{UE1}}^{\text{UL}} / \rho \right\} - \Pr \left\{ |h_{\text{BS, UE2}}|^2 - |h_{\text{BS, UE1}}|^2 \gamma_{\text{UE2}}^{\text{UL}} \geq \gamma_{\text{UE2}}^{\text{UL}} / \rho, |h_{\text{BS, UE1}}|^2 < \gamma_{\text{UE1}}^{\text{UL}} / \rho \right\} \\
&= 1 - \int_{\gamma_{\text{UE1}}^{\text{UL}} / \rho}^{+\infty} \int_0^{\frac{x - \gamma_{\text{UE1}}^{\text{UL}} / \rho}{\gamma_{\text{UE1}}^{\text{UL}}}} f_{|h_{\text{BS, UE2}}|^2}(y) f_{|h_{\text{BS, UE1}}|^2}(x) dy dx - \int_{\frac{\gamma_{\text{UE2}}^{\text{UL}} + \gamma_{\text{UE2}}^{\text{UL}} \gamma_{\text{UE1}}^{\text{UL}}}{\rho}}^{+\infty} \int_{\gamma_{\text{UE1}}^{\text{UL}} / \rho}^{\frac{x - \gamma_{\text{UE2}}^{\text{UL}} / \rho}{\gamma_{\text{UE2}}^{\text{UL}}}} f_{|h_{\text{BS, UE1}}|^2}(y) f_{|h_{\text{BS, UE2}}|^2}(x) dy dx \\
&= 1 - \frac{\beta_{\text{BS, UE1}} \exp\left(-\frac{\gamma_{\text{UE1}}^{\text{UL}}}{\beta_{\text{BS, UE1}} \rho}\right)}{\gamma_{\text{UE1}}^{\text{UL}} \beta_{\text{BS, UE2}} + \beta_{\text{BS, UE1}}} - \frac{\beta_{\text{BS, UE2}}}{\gamma_{\text{UE2}}^{\text{UL}} \beta_{\text{BS, UE1}} + \beta_{\text{BS, UE2}}} \exp\left(-\left(\frac{\gamma_{\text{UE1}}^{\text{UL}}}{\beta_{\text{BS, UE1}} \rho} + \frac{\gamma_{\text{UE2}}^{\text{UL}} + \gamma_{\text{UE2}}^{\text{UL}} \gamma_{\text{UE1}}^{\text{UL}}}{\beta_{\text{BS, UE2}} \rho}\right)\right), \quad (39)
\end{aligned}$$

$$P_{\text{out}, t_3}^{\text{UE2, UL}} = 1 - \frac{\beta_{\text{BS, UE2}} \exp\left(-\frac{\gamma_{\text{UE2}}^{\text{UL}}}{\beta_{\text{BS, UE2}} \rho}\right)}{\gamma_{\text{UE2}}^{\text{UL}} \beta_{\text{BS, UE1}} + \beta_{\text{BS, UE2}}} - \frac{\beta_{\text{BS, UE1}}}{\gamma_{\text{UE1}}^{\text{UL}} \beta_{\text{BS, UE2}} + \beta_{\text{BS, UE1}}} \exp\left(-\left(\frac{\gamma_{\text{UE2}}^{\text{UL}}}{\beta_{\text{BS, UE2}} \rho} + \frac{\gamma_{\text{UE1}}^{\text{UL}} + \gamma_{\text{UE1}}^{\text{UL}} \gamma_{\text{UE2}}^{\text{UL}}}{\beta_{\text{BS, UE1}} \rho}\right)\right). \quad (40)$$

$$R = \left(1 - P_{\text{out}}^{\text{UE1, DL}}\right) R_{\text{UE1}}^{\text{DL}} + \left(1 - P_{\text{out}}^{\text{UE2, DL}}\right) R_{\text{UE2}}^{\text{DL}} + \left(1 - P_{\text{out}, t_2}^{\text{UE1, UL}}\right) R_{\text{UE1}}^{\text{UL}} + \left(1 - P_{\text{out}, t_3}^{\text{UE1, UL}}\right) R_{\text{UE1}}^{\text{UL}} + \left(1 - P_{\text{out}}^{\text{UE2, UL}}\right) R_{\text{UE2}}^{\text{UL}}. \quad (43)$$

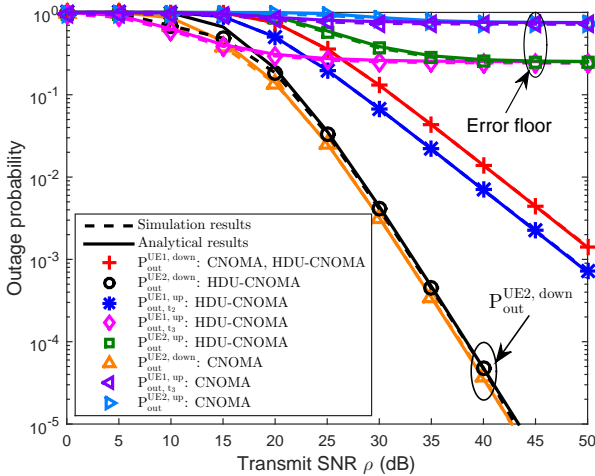


Fig. 3. Outage probability for the proposed HDU-CNOMA scheme and a conventional CNOMA scheme.

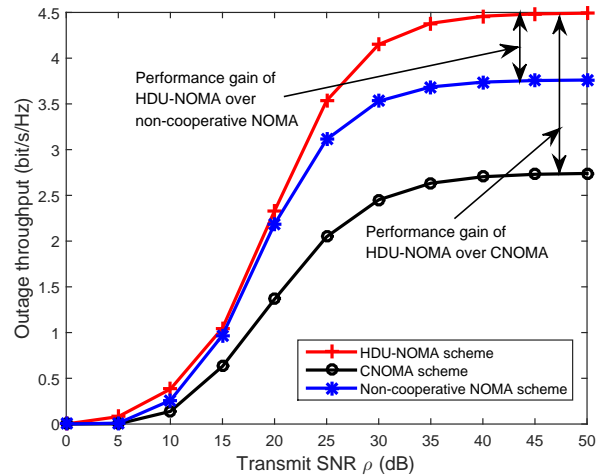


Fig. 4. Outage throughput (bits/s/Hz) for HDU-CNOMA scheme, conventional CNOMA scheme[14], and non-cooperative NOMA scheme.

IV. SIMULATION RESULTS

In this section, the performances of our proposed scheme are evaluated through simulations. Without loss of generality, we assume that the variances of channel coefficient are $\beta_{\text{BS, UE1}} = 1$, $\beta_{\text{BS, UE2}} = 0.05$, and $\beta_{\text{UE1, UE2}} = 0.8$. The target data rates are $R_{\text{UE1}}^{\text{DL}} = R_{\text{UE2}}^{\text{DL}} = R_{\text{UE1}}^{\text{UL}} = R_{\text{UE2}}^{\text{UL}} = 1$ bit/s/Hz and the power allocation factors are $\alpha_{\text{UE1}}^{t_1} = 0.05$, $\alpha_{\text{UE2}}^{t_1} = 0.95$, $\alpha_{\text{BS}}^{t_2} = 0.1$, and $\alpha_{\text{UE2}}^{t_2} = 0.9$. The approximation parameter for Gauss-Chebyshev integration is set as $n = 100$.

Figure 3 illustrates the simulation results and analytical results for the outage probability of conventional CNOMA scheme and our proposed HDU-CNOMA scheme. Note that the outage probability for $P_{\text{out}}^{\text{UE1, DL}}$ is the same for both CNOMA and HDU-CNOMA schemes. It can be observed that our analytical results closely match with the simulation

results, especially for the high SNR regime. Compared to the CNOMA scheme, $P_{\text{out}}^{\text{UE2, DL}}$ of our proposed scheme is slightly higher due to the power loss in the cooperative phase. The gap on $P_{\text{out}}^{\text{UE2, DL}}$ between CNOMA and HDU-CNOMA can be further reduced by allocating a higher transmit power for UE 2 than that of the BS during the cooperative phase to maintain the signal reception reliability at UE 2. On the other hand, although only a small fraction of power is allocated for uplink transmission during t_2 in HDU-CNOMA scheme, it has a lower outage probability than that of uplink NOMA transmissions in t_3 , especially for high SNR regime. This is due to the fact that the side information s_2 assists the BS to cancel the interference in the superimposed signal transmitted during the cooperative phase. For $R_{\text{UE1}}^{\text{UL}} = R_{\text{UE2}}^{\text{UL}} > \frac{1}{2}$ bit/s/Hz, we can observe the error floor of $P_{\text{out}, t_3}^{\text{UE1, UL}}$ and $P_{\text{out}}^{\text{UE2, UL}}$ for

both CNOMA and HDU-NOMA schemes, which validates our derivations in (42). Also, it can be observed that our proposed scheme results in a lower error floor than that of the CNOMA scheme. This is because our proposed scheme exploits two time slots, t_2 and t_3 , for UE 1 to transmit the target data rate $R_{\text{UE1}}^{\text{UL}}$ while CNOMA only transmits in t_3 .

Figure 4 depicts the outage throughput for all the schemes shown in Figure 2. It can be observed that our proposed scheme achieves the largest outage throughput. In particular, the proposed scheme offers substantial performance gains over the two baseline schemes in the moderate to high SNR regime. Although the superimposed transmission of the proposed scheme during cooperative phase slightly degrades the received signal quality at UE 2, the performance gain brought by the extra interference-free uplink transmission of UE 1 outweighs the performance loss at UE 2 which increases the overall system outage throughput. In contrast, the CNOMA scheme has a lowest outage throughput due to the following two reasons. First, compared to the proposed HDU-CNOMA scheme, the CNOMA scheme does not fully exploit the degrees of freedom in the system for uplink and downlink communications. Second, compared to the non-cooperative NOMA scheme, the performance of the CNOMA scheme relies on the existence of short range communication between the strong user and the weak user [14] which does not always exist in practical systems.

V. CONCLUSION

In this paper, a novel HDU-CNOMA scheme was proposed to increase the spectral efficiency and to achieve a better trade-off between signal reception reliability and spectral efficiency for cooperative NOMA systems. Particularly, the cooperative transmission and uplink transmission were integrated during the cooperative phase, and the side information at the BS was utilized to obtain an additional interference-free uplink transmission. To evaluate the performance of our proposed scheme, we analyzed the corresponding outage probability, diversity order, and system outage throughput. Simulations were conducted to verify our analytical results. With only a slightly performance degradation on the signal reception reliability at the weak user, our proposed scheme provides a substantial improvement on system spectral efficiency over a conventional cooperative NOMA scheme and a non-cooperative NOMA scheme.

REFERENCES

- [1] V. W. S. Wong, R. Schober, D. W. K. Ng, and L.-C. Wang, *Key Technologies for 5G Wireless Systems*. Cambridge university press, 2017.
- [2] L. Dai, B. Wang, Y. Yuan, S. Han, I. Chih-Lin, and Z. Wang, "Non-orthogonal multiple access for 5G: solutions, challenges, opportunities, and future research trends," *IEEE Commun. Mag.*, vol. 53, no. 9, pp. 74–81, Sep. 2015.
- [3] Z. Wei, J. Yuan, D. W. K. Ng, M. Elkashlan, and Z. Ding, "A survey of downlink non-orthogonal multiple access for 5G wireless communication networks," *ZTE Communications*, vol. 14, no. 4, pp. 17–25, Oct. 2016.
- [4] L. Song, Y. Li, Z. Ding, and H. V. Poor, "Resource management in non-orthogonal multiple access systems: State of the art and research challenges," *arXiv preprint arXiv:1610.09465*, 2016.
- [5] Z. Ding, Z. Yang, P. Fan, and H. Poor, "On the performance of non-orthogonal multiple access in 5G systems with randomly deployed users," *IEEE Signal Process. Lett.*, vol. 21, no. 12, pp. 1501–1505, Dec. 2014.

- [6] Z. Yang, Z. Ding, P. Fan, and G. K. Karagiannidis, "On the performance of non-orthogonal multiple access systems with partial channel information," *IEEE Trans. Commun.*, vol. 64, no. 2, pp. 654–667, Feb. 2016.
- [7] Y. Sun, D. W. K. Ng, Z. Ding, and R. Schober, "Optimal joint power and subcarrier allocation for full-duplex multicarrier non-orthogonal multiple access systems," *IEEE Trans. Commun.*, 2017, accepted for publication.
- [8] S. Timotheou and I. Krikidis, "Fairness for non-orthogonal multiple access in 5G systems," *IEEE Signal Process. Lett.*, vol. 22, no. 10, pp. 1647–1651, Oct. 2015.
- [9] Y. Liu, M. Elkashlan, Z. Ding, and G. K. Karagiannidis, "Fairness of user clustering in MIMO non-orthogonal multiple access systems," *IEEE Commun. Lett.*, vol. 20, no. 7, pp. 1465–1468, Jul. 2016.
- [10] J. N. Laneman, D. N. C. Tse, and G. W. Wornell, "Cooperative diversity in wireless networks: Efficient protocols and outage behavior," *IEEE Trans. Inf. Theory*, vol. 50, no. 12, pp. 3062–3080, Dec. 2004.
- [11] X. Chen, C. Zhong, C. Yuen, and H. H. Chen, "Multi-antenna relay aided wireless physical layer security," *IEEE Commun. Mag.*, vol. 53, no. 12, pp. 40–46, Dec. 2015.
- [12] J. Zhang, L. Dai, Y. Zhang, and Z. Wang, "Unified performance analysis of mixed radio frequency/free-space optical dual-hop transmission systems," *J. Lightwave Technol.*, vol. 33, no. 11, pp. 2286–2293, Jun. 2015.
- [13] D. W. K. Ng and R. Schober, "Cross-layer scheduling for OFDMA amplify-and-forward relay networks," *IEEE Trans. Veh. Technol.*, vol. 59, no. 3, pp. 1443–1458, Mar. 2010.
- [14] Z. Ding, M. Peng, and H. Poor, "Cooperative non-orthogonal multiple access in 5G systems," *IEEE Commun. Lett.*, vol. 19, no. 8, pp. 1462–1465, Aug. 2015.
- [15] J. Men and J. Ge, "Non-orthogonal multiple access for multiple-antenna relaying networks," *IEEE Commun. Lett.*, vol. 19, no. 10, pp. 1686–1689, Oct. 2015.
- [16] Z. Zhang, Z. Ma, M. Xiao, Z. Ding, and P. Fan, "Full-duplex device-to-device aided cooperative non-orthogonal multiple access," *IEEE Trans. Veh. Technol.*, vol. PP, no. 99, pp. 1–1, Aug. 2016.
- [17] J. B. Kim and I. H. Lee, "Non-orthogonal multiple access in coordinated direct and relay transmission," *IEEE Commun. Lett.*, vol. 19, no. 11, pp. 2037–2040, Nov. 2015.
- [18] C. Zhong and Z. Zhang, "Non-orthogonal multiple access with cooperative full-duplex relaying," *IEEE Commun. Lett.*, vol. 20, no. 12, pp. 2478–2481, Dec. 2016.
- [19] J. Cui, Z. Ding, and P. Fan, "A novel power allocation scheme under outage constraints in NOMA systems," *IEEE Signal Process. Lett.*, vol. 23, no. 9, pp. 1226–1230, Sep. 2016.
- [20] J. B. Kim and I. H. Lee, "Capacity analysis of cooperative relaying systems using non-orthogonal multiple access," *IEEE Commun. Lett.*, vol. 19, no. 11, pp. 1949–1952, Nov. 2015.
- [21] Z. Wei, D. W. K. Ng, and J. Yuan, "Power-efficient resource allocation for MC-NOMA with statistical channel state information," *Proc. IEEE Global Commun. Conf.*, pp. 1–1, Dec. 2016.
- [22] D. Tse and P. Viswanath, *Fundamentals of wireless communication*. Cambridge university press, 2005.
- [23] F. B. Hildebrand, *Introduction to numerical analysis*. Courier Corporation, 1987.
- [24] D. N. C. Tse, P. Viswanath, and L. Zheng, "Diversity-multiplexing tradeoff in multiple-access channels," *IEEE Trans. Inf. Theory*, vol. 50, no. 9, pp. 1859–1874, Sep. 2004.
- [25] Z. Yang, Z. Ding, P. Fan, and N. Al-Dhahir, "A general power allocation scheme to guarantee quality of service in downlink and uplink noma systems," *IEEE Transactions on Wireless Communications*, vol. 15, no. 11, pp. 7244–7257, Nov. 2016.